PROJECT REPORT ON

DESIGN & SIMULATION OF A

PIEZOELECTRICITY GENERATION SYSTEM

PRESENTED BY

AGHEYISI IYOSAYI: ENG2002416

ASOYA DAVID KELECHI: ENG2002428

AKPOROKAH EMMANUEL: ENG2002422

SUBMITTED TO

THE DEPARTMENT OF MECHANICAL ENGINEERING,

FACULTY OF ENGINEERING.

UNIVERSITY OF BENIN, BENIN CITY.

CERTIFICATION

We hereby certify that this project titled “Design and Simulation of a Piezoelectric Generation System” was carried out by Agheyisi Iyosayi, Asoya David and Akporokah Emmanuel, students of the Department of Mechanical Engineering, University of Benin. This project was submitted in partial fulfillment of the requirements for the award of B.ENG Mechanical Engineering.

This is also to certify that this project was carried out under the supervision of Engr. Dr. Omo-Oghogho. He provided guidance and direction through the course of this project work.

This project is an original copy of ours and has not been submitted in part or full for the award of any other degree or at any other institution.

……. **Date: .....**

Engr. Dr Omo Oghogho
Project Supervisor

……. **Date: .....**

Engr. Martins Osikhuemhe
Project Coordinator

…….. **Date: .....**

Prof. Engr. Òsarobo Ighodaro
Head of Department

DEDICATION

We dedicate this report to God Almighty, whose grace has granted us the strength to accomplish all that was necessary for the success of this project. To our families, whose unwavering support and encouragement have been the foundation of our academic journey. To the Department of Mechanical Engineering, whose guidance and commitment to equipping us through extensive training and lectures have been pivotal in shaping us into who we are today. This work is also dedicated to all who have inspired and supported us along the way. Your faith in our potential has ignited our passion for learning and striving for excellence.

ACKNOWLEDGEMENTS

We express our deepest gratitude to our project supervisor, Engr. Dr. Omo-Oghogho for his insightful guidance, unwavering support, and constructive criticism throughout the entirety of this project.

We would also like to acknowledge the Department of Mechanical Engineering at the University of Benin for providing the necessary academic environment and resources that made this work possible.

Finally, we extend our sincere thanks to our families and colleagues for their patience, encouragement, and support. This work is a testament to their continuous belief in our abilities.

ABSTRACT

This project presents the design and simulation of a modular piezoelectric energy-harvesting system to evaluate it's potential as an alternative sustainable power source, particularly from human foot traffic in high-density areas. Using MATLAB and Simulink, the study employed a Model-Based Design approach to analyse the influence of three critical design factors: footstep force magnitude, the number of stacked crystals, and piezoelectric material selection.

The findings provide data-driven insights concluding that maximising energy output requires prioritising materials with a high piezoelectric voltage constant, optimising crystal stacking, and deploying the harvester in high-impact locations.

TABLE OF CONTENTS

LIST OF FIGURES AND TABLES

TABLES

FIGURES

CHAPTER ONE

1.1. INTRODUCTION

As global energy demands continue to rise, the search for alternative and sustainable energy sources has become a critical area of research. According to the International Energy Agency's (IEA) *New Policies Scenario*, global electricity demand is projected to increase by approximately 80% between 2012 and 2040 (Elhalwagy et al., 2017). This growing demand, coupled with environmental concerns related to fossil fuel consumption, has driven significant interest in renewable and clean energy technologies.

Among the various emerging energy solutions, piezoelectric energy harvesting has gained attention as a promising approach to generating electricity from everyday human activities, such as walking. Piezoelectricity refers to the ability of certain materials to generate an electrical charge when subjected to mechanical stress. This phenomenon is particularly useful for harvesting energy from human movement, specifically footsteps. Footstep power generation utilizes piezoelectric materials embedded in floors to convert kinetic energy into electrical energy. In high-footfall areas such as train stations, shopping malls, pedestrian walkways, and university campuses, the cumulative energy generated from footsteps can be significant (Elhalwagy et al., 2017). If effectively captured and stored, this energy could power small electronic devices, lighting systems, and digital displays—contributing to sustainable urban infrastructure.

The efficiency of piezoelectric footstep power generation systems depends on several factors, including the output power per step, energy storage mechanisms, cost-effectiveness, and distribution of foot traffic. Optimizing the placement of piezoelectric materials in areas with high pedestrian density further enhances energy collection efficiency. For practical applications, the

harvested power can be used as a primary source or as a supplementary supply to trigger low-energy sensors and power small electronics (Elhalwagy et al., 2017).

The phenomenon of piezoelectricity, first discovered in the 19th century, is based on the ability of certain materials to generate an electric charge in response to mechanical deformation. This effect is reversible in that when an electric field is applied, these materials can also undergo mechanical deformation. These materials include crystals such as quartz, topaz, tourmaline, Rochelle salt, as well as engineered ceramics and polymers such as barium titanate, lead zirconate titanate (PZT), and polyvinylidene fluoride (PVDF).

Piezoelectricity -more in depth- is the property of certain crystalline and ceramic materials to generate an electric charge when subjected to mechanical stress, and conversely, to undergo mechanical deformation when exposed to an external electric field. The term is derived from the Greek word *piezein*, meaning "to press," reflecting its fundamental principle of converting mechanical energy into electrical energy and vice versa. This phenomenon arises from the unique internal structure of piezoelectric materials, in which the arrangement of atoms lacks a center of symmetry. When mechanical stress is applied, the displacement of positive and negative charge centers within the crystal lattice leads to the development of an electric potential across the material. In the reverse effect, applying an electric field realigns the internal dipoles, producing a measurable change in shape or dimension. The phenomenon by which certain materials generate an electric charge when subjected to mechanical stress and, conversely, experience mechanical deformation when exposed to an electric field is referred to as the Piezoelectric Effect.

The Piezoelectric effect is widely encountered in nature and many synthetic materials. The best known natural piezoelectric material is quartz, SiO_2, while among thousands of synthetic

materials, the most widely used and best understood are ferroelectric ceramics belonging to solid solutions of lead zirconate and lead titanate, $Pb(Zr,Ti)O_3$ (PZT). Quartz exhibits nearly perfect, unhysteretic, linear and stable, but a weak piezoelectric response. The piezoelectric coefficients of PZT are about two orders of magnitude higher than in quartz (Table 1). At present, PZT is not available in single crystal form; it is prepared as ceramics that need to be poled to exhibit the piezoelectric response. The best piezoelectric properties in PZT are observed near 1:1 Zr: Ti ratio. In this region (called morphotropic phase boundary region or MPB), the crystal structure of PZT changes from tetragonal ($PbTiO_3$-rich side) to rhombohedral ($PbZrO_3$-rich side) via an intermediary monoclinic structure (Figure 1.1).

Table 1.1

Material	***Piezoelectric coefficient*** **(pCN^{-1})**	***Coupling coefficient***	***Comment***
Soft PZT	d_{33}=600	k_{33}=0.75	Poled ceramic
Hard PZT	d_{33}=200	k_{33}=0.67	Poled ceramic
	d_{15}=500		
PMN-PT	d_{33}=2500	k_{33}=0.93	Single crystal; d_{33} long [0 0 1] pseudo-cubic direction
	d_{15}=4900		
SiO_2	d_{11}=2.3	k_{11}=0.1	Single crystal
PVDF	d_{31}=30	k_{33}=0.2	Poled polymer
	d_{33}=−15		

Piezoelectric properties of selected materials (2005, Encyclopedia of Condensed Matter Physics, D. Damjanovic)

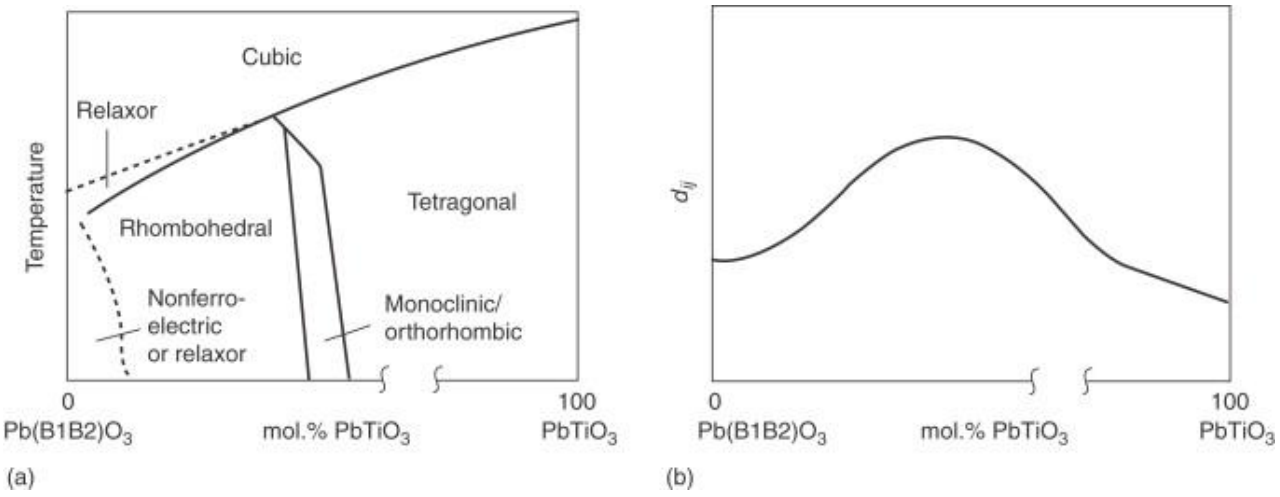

Figure 1.1: Schematic illustration of (a) temperature-composition phase diagram, and (b) piezoelectric coefficient–composition dependence, as observed in many solid solutions of simple and complex perovskites (e.g., $PbZrO_3$ and $Pb(Mg_{1/2}Nb_{2/3})O_3$) with $PbTiO_3$. (2005, Encyclopedia of Condensed Matter Physics, D. Damjanovic)

Recently, a new class of piezoelectric crystals was discovered with longitudinal and transverse piezoelectric coefficients reaching, along certain crystallographic directions, values of 1000–2500 pC N^{-1} with shear coefficients in the range 4000–5000 pC N^{-1}, and coupling coefficients as large as 0.95. These crystals are solid solutions of a relaxor ferroelectric, such as $Pb(Zn_{1/2}Nb_{2/3})O_3$ or $Pb(Mg_{1/2}Nb_{2/3})O_3$, and ferroelectric $PbTiO_3$. As in PZT, the properties are maximized in the vicinity of the MPB, and along certain crystallographic directions, as shown in Figure 2. When a crystal is poled along a nonpolar direction, a special domain structure results, which is referred to as "engineered domain structure." In some cases, (e.g., rhombohedral crystals poled along 〈0 0 1〉 pseudo-cubic direction, Figure 1.2), the engineered domain state not only gives a large piezoelectric response but is also stable and hysteresis free.

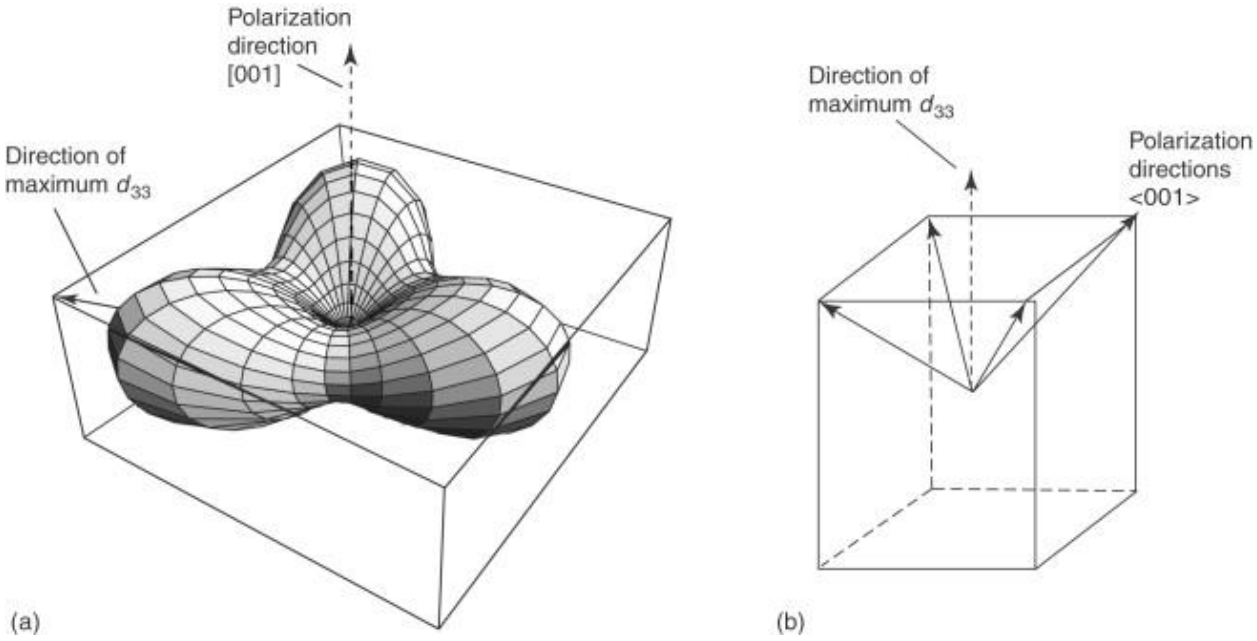

Figure 1.2. Dependence of the longitudinal d33 piezoelectric coefficient on crystal orientation for (a) crystals belonging to point group 3m, such as rhombohedral PZT, $BaTiO_3$, or $Pb(Zn_{1/2}Nb_{2/3})O_3$-$PbTiO_3$, (b) the four domain states in such a crystal poled along pseudo-cubic [0 0 1] direction. (2005, Encyclopedia of Condensed Matter Physics, D. Damjanovic)

Polymer–ceramic piezoelectric composites, which have been developed during the 1970s and 1980s, are now routinely used for medical imaging and underwater (SONAR) applications. The polymer phase is non-piezoelectric while ceramic is a PZT composition. Different connectivities of the two phases are used. The role of the polymer is mainly to reduce the density and thus improve acoustical impedance matching to human body and water, and to reduce transverse piezoelectric effect and thus reduce cross-talk of elements in transducer arrays. The most important synthetic organic piezoelectric is PVDF.

PZT, quartz, and PVDF are the most widely used piezoelectric materials. Other than these materials, $LiNbO_3$ and $LiTaO_3$, tourmaline, modified $PbTiO_3$, lead metaniobate $PbNb_2O_6$,

$BaTiO_3$, and materials belonging to the family of bismuth titanate-based aurivillius structures are used for special applications. There are some attempts to partly replace quartz by crystals belonging to the Langasite $La_3Ga_5SiO_{14}$ family, and $GaPO_4$, both of which exhibit a higher piezoelectric response than quartz, temperature-stable properties and operating temperatures significantly higher than quartz. Recent developments in the area of piezoelectric thin films have raised interest in PZT and AlN films. Presently, there are attempts to develop lead-free piezoelectric materials (e.g., $KNbO_3$, $Na_{0.5}Bi_{0.5}TiO_3$ based compositions) with properties comparable to those of PZT. The *ab initio* theories appear to be a promising approach in predicting new materials with high piezoelectric properties.

Many organic, synthetic and natural, and biological materials are piezoelectric, including nylon, wood, hair, bones, and eye tissue. The piezoelectric effect in bovine eyes is several times higher than in quartz. The origin of piezoelectricity in animal and human tissue can be traced to collagen. However, presently, it is not clear whether the piezoelectric effect in living tissue has any physiological role. (2005, Encyclopedia of Condensed Matter Physics, D. Damjanovic)

In modern contexts, piezoelectric systems are being explored for applications ranging from wearable electronics to smart infrastructure, where ambient vibrations, pressure, or movement can be transformed into electrical energy. The simplicity, compact size, and solid-state nature of piezoelectric devices make them ideal for integration into a wide range of mechanical systems without significantly altering the design or increasing energy consumption. In the context of this project, the study and application of piezoelectric generation will focus on understanding the underlying material properties and system design considerations that influence energy harvesting performance.

1.2. PROJECT STATEMENT

This project focuses on the simulation-based analysis of a modular piezoelectric energy-harvesting system, aimed at evaluating how mechanical energy from everyday human and environmental activities can be efficiently converted into usable electrical power. Potential mechanical energy sources include foot traffic in high-density urban areas, pedestrian walkways, large event venues, transportation hubs, and other locations with frequent human movement.

The research models a modular piezoelectric harvester using MATLAB and Simulink, with emphasis on analyzing how design parameters influence performance. Three main factors are investigated: the effect of varying footstep force magnitudes, the impact of stacking multiple piezoelectric crystals, and the role of material selection based on piezoelectric constants. Together, these factors determine the voltage, power, and total energy that can be harvested from each footstep.

The performance of the system will be evaluated in MATLAB and Simulink through simulated footstep loading scenarios, comparing the total power output and the average energy harvested per piezoelectric element. The simulations will also investigate the effect of stacking multiple piezoelectric crystals on each unit to determine its influence on overall output power.

Ultimately, this simulation study aims to identify the most effective design parameters for piezoelectric energy harvesting from footfall, focusing on the influence of force magnitude, crystal stacking, and material selection. The insights gained are intended to guide the development of practical, efficient, and scalable systems that can be deployed in high-traffic

urban areas and off-grid environments, where reliable supplementary energy sources are most needed.

1.3. AIM AND OBJECTIVES

1.3.1. AIM: The primary aim of this project is to simulate, analyze, and optimize a piezoelectric energy-harvesting system using MATLAB and Simulink. The study focuses on evaluating how key design parameters—such as footstep force magnitude, crystal stacking, and piezoelectric material selection—influence energy conversion efficiency. By examining total power output, average energy harvested per crystal, and the effect of multiple stacked configurations, the project seeks to provide data-driven insights that support the development of efficient, scalable, and practical piezoelectric harvesters. Special emphasis is placed on their potential as sustainable, supplementary energy sources in high-traffic urban areas and off-grid locations where conventional power supply is limited or unavailable.

1.3.2. Objectives:

1. To develop a MATLAB/Simulink simulation model of a piezoelectric footstep energy harvester for quantitative performance analysis.
2. To generate realistic footstep force profiles and evaluate their effect on harvested power and total energy output.
3. To assess overall system efficiency by comparing energy output across force magnitudes, stacking levels, and material types, and to identify optimal design parameters for real-world application in high-traffic or off-grid environments.

1.4. SCOPE OF THE PROJECT

The scope of this project covers the theoretical study, simulation modeling, material selection, and performance evaluation of a piezoelectric footstep energy-harvesting system. The work is structured into key phases, each addressing critical aspects of system efficiency and feasibility:

1. **Simulation Modeling** – Development of a MATLAB/Simulink model representing the electromechanical coupling of piezoelectric crystals subjected to footstep loading conditions.
2. **Force Profile Studies** – Generation and analysis of realistic footstep force profiles to evaluate how variations in footstep magnitude affect harvested voltage, power, and total energy.
3. **Stacking Analysis** – Investigation of the impact of stacking multiple piezoelectric crystals on system performance, with attention to energy gains and diminishing returns.
4. **Material Comparison** – Integration of selected piezoelectric materials (PZT-5A, PZT-5H, BT, PVDF, PMN-PT) into the model to assess how material properties influence energy output.
5. **Performance Evaluation** – Comparative assessment of total harvested energy, average output per crystal, and efficiency across different forces, stacking levels, and materials to identify optimal design parameters for real-world applications.

CHAPTER TWO

LITERATURE REVIEW

2.1. WORKING PRINCIPLE AND THEORETICAL FUNDAMENTALS

Electrical energy can be harvested from footsteps through the piezoelectric effect. This method converts mechanical energy from footfalls into usable electrical power, making them viable for energy harvesting in high-foot-traffic areas.

2.1.1. Piezoelectric-Based Smart Floor Solutions

A widely studied approach to footstep power generation is the piezoelectric-based smart floor system shown in the figure below (Puscasu et al., 2018). This system utilizes piezoelectric materials that generate an electric charge when subjected to mechanical stress. The design typically consists of flooring layers with a floating surface suspended by springs above piezoelectric elements. When a pedestrian step on the floor, the surface depresses, causing contact between projections on the tile and the piezoelectric material. The applied force induces mechanical strain within the piezoelectric material, which results in charge generation.

The system is designed to ensure durability and efficiency. The springs provide stability, preventing excessive deformation of the piezoelectric material, which could lead to damage. A

base plate securely fitted into the frame provides additional support and distributes pressure evenly

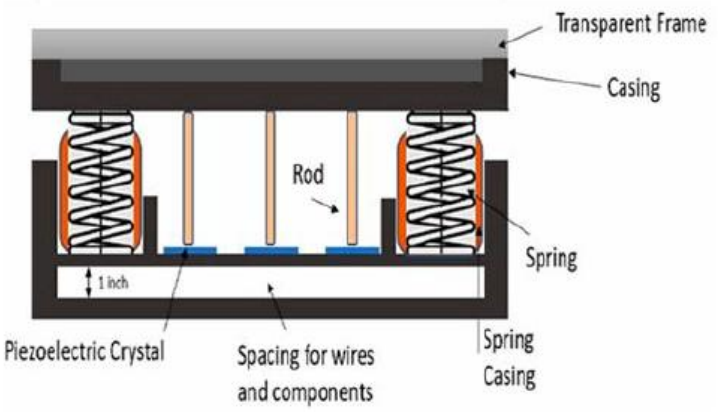

Figure 2.1. General approach to piezoelectric footstep power generation (Shanmugam et al. ,2020).

The piezoelectric effect is the core principle behind this mechanism. It describes the generation of electrical charge in solid materials—such as crystals, ceramics, or some polymers—when subjected to mechanical stress. The effect is reversible, meaning an applied electric field can also induce mechanical deformation in these materials.

At the atomic level, the process works as follows:

1. In crystalline materials with an asymmetric charge distribution, mechanical stress causes charge displacement, resulting in electrical polarization.
2. This polarization creates a voltage difference across the material, allowing the generation of electrical power (Gupta et al., 2014).
3. The amount of charge generated is directly proportional to the applied mechanical force.

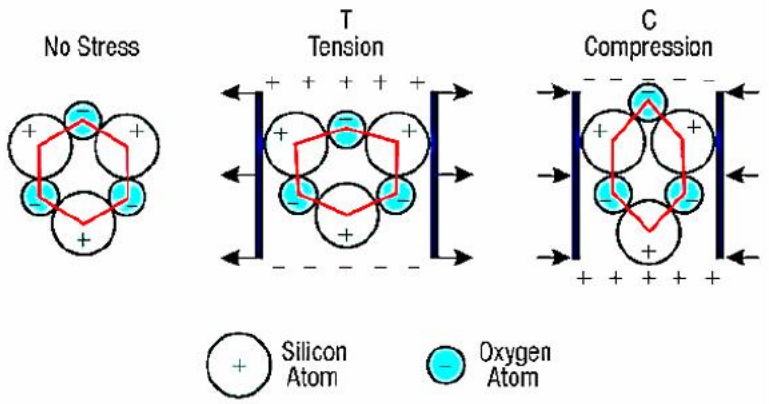

Figure 2.2. Piezoelectric effect in quartz (General approach to piezoelectric footstep power generation (Shanmugam et al. ,2020)).

2.1.2. Piezoelectric Materials and Their Properties

Piezoelectric materials can be either natural or synthetic, with some common examples including:

1. Natural Quartz Crystals
2. Polycrystalline Piezo-Ceramics
3. Polyvinylidene Fluoride (PVDF) Polymers
4. Bone and Wood (Biological Piezoelectric Materials)

The effectiveness of a piezoelectric material depends on its chemical structure and poling process. In polycrystalline ceramics, individual dipole domains must be aligned through poling to exhibit macroscopic piezoelectricity. The generated charge is directly proportional to the applied mechanical stress.

In practical applications, piezoelectric smart floors are embedded with an array of piezoelectric elements connected in parallel or series to optimize power output. The generated AC voltage is then rectified and stored in batteries or used to power small electronic devices.

2.1.3. Commercial Smart-Floors and Components for Energy-Harvesting Applications

The rapidly growing market for energy harvesting systems is poised for significant growth, expected to rise from USD 468 million in 2021 to USD 701 million by 2026, reflecting a compound annual growth rate (CAGR) of 8.4%. This growth is driven by several factors, including the increasing demand for sustainable, energy-efficient, low-maintenance systems and the rising adoption of Internet of Things (IoT) devices in automation systems. Furthermore, favorable government initiatives and the widespread adoption of wireless sensor networks (WSNs) integrated with energy harvesting technologies are shaping the future of the sector. In particular, energy harvesting systems are being deployed across various applications in the construction, residential, and industrial automation sectors, with the United States emerging as a leading hub for these innovations. Meanwhile, Europe remains a central player in the manufacturing of energy harvesting systems, housing some of the most prominent enterprises in the field, such as ABB,

Linear Technology, ST Microelectronics, and Honeywell (MarketsandMarkets, 2021).

The integration of energy-harvesting technologies in smart floors offers tremendous promise for generating off-grid power, especially in high-footfall areas like urban environments, transport hubs, and public spaces. These systems transform kinetic energy generated from human footfalls into usable electrical energy. Several commercial smart-floor technologies have been developed and are now being deployed across various sectors, such as public infrastructure, education, retail, and sports. Below are some notable examples of these innovative systems and their capabilities:

1. Pavegen Tiles

Pavegen is a pioneering device developed by Laurence Kemball-Cook that captures kinetic energy from human footfalls, converting it into electrical energy. The project began in 2008, and over the years, more than 750 prototypes have been created. The tiles are designed to be integrated into both outdoor and indoor pavements, converting the small vertical displacement (up to 5 mm) produced by foot traffic into energy. Each tile consists of piezoelectric blocks and an electromagnetic generator arranged in a triangular pattern. The system captures mechanical energy from the pressure exerted by human footsteps and transforms it into electrical energy that can power applications such as pedestrian lighting, public illumination, traffic signals, and outdoor advertising (Kemball-Cook, 2013).

Pavegen tiles have been deployed in several high-profile locations, including local football fields in Brazil and Nigeria, where they have been used to generate power for various community services. In 2013, Pavegen installed its kinetic tiles along the final stretch of the Paris Marathon.

The 40,000 participants in the event collectively generated 7 kWh of energy as they crossed the finish line, powering LED lighting along the route. These tiles are particularly suited for high-traffic areas such as transport hubs, busy streets, and public events, providing an innovative and sustainable solution for generating energy in urban environments (Pavegen, 2013).

Figure 2.3. Pavegen tiles installation (Pavegen, 2013).

2. Smart Energy Floor by Energy Floors

The Smart Energy Floor® (SEF) is a product developed by Energy Floors, marking a significant advancement in the integration of energy harvesting with floor systems. The SEF can generate between 2–20 Joules per step, depending on factors such as user weight, movement type, and the maximum deflection of the floor module. Each tile has a size of 500x500x100 mm^3, with the core made from sustainable materials such as recycled ceramics, rubber, glass, bamboo, or synthetic composites. The SEF has a maximum static load of 25 kN, making it suitable for various applications, including both pedestrian and vehicular use (Energy Floors, 2018).

The Smart Energy Floor® was developed in several versions, including the "Dancer," "Gamer,"

and "Walker" models, each designed with specific user demographics and application scenarios in mind. The "Dancer" model, for example, uses an electromechanical solution based on a rackpinion mechanism that converts linear tile motion into rotational movement to drive an] electromagnetic generator. It is capable of producing up to 35 W of power per tile. The "Walker" model integrates walkable solar modules with a built-in LED illumination system, while the "Gamer" model is designed for use in educational and fitness environments, promoting health through interactive engagement (Energy Floors, 2018).

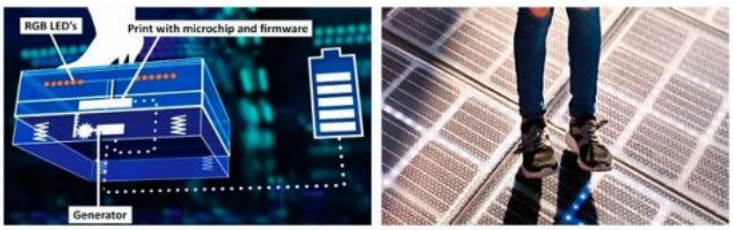

Figure 2.4. Sustainable energy floor (Energy Floors, 2018).

3. POWERleap Tiles

POWERleap, developed by E. Redmond as part of her thesis at the University of Michigan, is another innovative floor solution for smart sensing and power generation. This system utilizes piezoelectric generators to harvest energy from human footsteps, a method that eliminates the need for moving components found in traditional mechanical systems like micro-turbines. The tiles employ piezoelectric materials such as polyvinylidene fluoride (PVDF) or lead zirconate titanate (PZT), which generate an electrical current when subjected to mechanical stress.

The tile design incorporates multiple layers of piezoelectric material arranged in a stack configuration, with electrodes made of copper, aluminum, or conductive ink. These electrodes collect the electrical charge generated by foot traffic. Additionally, each tile includes a Bluetooth transceiver to transmit data on the harvested power to an external receiver. The tiles can generate approximately 10 W/m² per hour, translating to about 1 kWh of energy for every 100 square meters of tile area with 3,000 to 5,000 people passing over it per hour. This technology can be used in various environments, from retail spaces to public transport stations, where high foot traffic makes it an effective means of energy harvesting (Redmond, 2021).

Figure 2.5. POWERleap tiles installation (Redmond, 2021).

Research into piezoelectric energy harvesting has grown rapidly, with many studies exploring ways to maximize energy conversion efficiency for specific applications. Asef Ishraq Sadaf et al (2024) conducted a detailed investigation into vibration-based energy harvesting using PZT-4 piezo-ceramic materials. In this study, a cantilever beam configuration was used, with comparative tests performed on beams with and without a tip mass. The results clearly showed that incorporating a tip mass lowered the resonant frequency and increased deflection amplitude, which in turn enhanced strain within the piezoelectric material and increased electrical output. The work also highlighted the importance of impedance matching between the piezoelectric source and the electrical load, as maximum power transfer was achieved when these impedances were closely matched.

Maung (2022) explored a different application by investigating footstep-based piezoelectric energy harvesting. In this study, piezoelectric discs were embedded beneath a walking surface, and various series and parallel electrical configurations were tested. The research found that connecting discs in series increased voltage output, while parallel connections improved current output. The mechanical arrangement of the discs also influenced performance, with configurations that applied force more directly to the active area of the material yielding better results. Although the harvested energy from individual footsteps was relatively small, the study demonstrated that cumulative energy from high-traffic areas could potentially be harnessed to power low-energy devices such as LED indicators or small wireless transmitters.

Beeby et al. (2007) studied energy harvesting by placing a coil at the end of a cantilever overhang excited by the base and oscillating between two magnets. They presented a small

volume electromagnetic generator (component volume 0.1 cm3, practical volume 0.15 cm3) optimised for harvesting by vibration from low level ambient vibration based on real application data. The generator produced useful power of 46 μW to a resistive load of 4 kΩ from a vibration level of 60 mg (g = 9.81 m/s2), when the electromagnetic device was shaken at a resonant frequency of 52 Hz. The generator delivered 30 % of the total power dissipated in the generator to electrical power in the load. From the basic equations governing electromagnetic generators, they concluded that the energy decreases with device volume, and reducing input vibration acceleration.

Li et al. (2000) developed a vibration harvesting power generator with a total volume of l cm3 using a laser micro machined resonant copper spring based on Faraday's Law of induction according to which a spring can convert mechanical energy into useful electrical power. Using innovative designs, the mass can be vibrated horizontally while the vibration input is applied vertically. The substantially horizontal vibration provides the highest output voltage of the generator. Li et al. developed a generator capable of producing a voltage of 2 V DC with 64 Hz to 120 Hz input frequency at 250 to 100 μm vibration amplitude.

Williams et al. (2001) developed a design methodology for linear micro-generators, where the design was applied to a millimetre scale microwave electromagnetic generator. The manufacture of a prototype device is described using generally available micro fabrication techniques. The results of the testing of the device in relation to a source of variable amplitude vibrations, in a vacuum and in air, are presented. With the device prototype, the electric power generation from mechanical vibration power was 0.3 μW at an excitation frequency of 4 MHz. The energy generated by such devices is proportional to the mass and vibration acceleration and inversely

proportional to resonant frequency as well as mechanical (electrical) damping factor. This means that more power can be extracted if the inertial mass is increased or the generator can work in the environment where the vibration level is high. To maximize the power that may be produced in any particular application, the resonant frequency of the generator must be designed to match the frequency range of the vibration source, and the maximum possible deformation of the device should be as great as possible. They concluded that mechanical damping is a dominant limiting factor in these devices and significant improvements in the output power can be achieved through better linearity of the spring and the load operation. Electromagnetic coupling also needs to be optimized to ensure a good impedance match between the device and the electric load.

Wang et al. (2012) designed, simulated, fabricated and characterized a micro electromagnetic vibration energy harvester with sandwiched structure and air channel. The harvester consists of the lower coil, an upper coil, an NdFeB permanent magnet and a plane of nickel with the spring integrated frame of silicon. The natural frequency of the magnet-spring system tested is 228.2 Hz. Comparison of the natural results tested and simulation shows that the micro electroplated Ni film Young's modulus is about 163 GPa rather than 210 GPa of bulk Ni material. These experimental results show that the air channel in the silicone frame of the prototype and the sandwiched structure are able to increase the induced voltage to 42 % of the single coil. The prototype has a resonant frequency of 280.1 Hz at an acceleration of 8 m/s2 which results from the nonlinear magnet-spring system. The prototype at resonant frequency of 280.1 Hz and 8 m/s2 input vibration acceleration generated 162.5 mV charging voltage. The maximum charging power obtained was approximately 21.2 μW corresponding to 66.25 μW/cm3 when the optimum load resistance was 81 Ω.

Chiu et al. (2010) analysed and modelled the nonlinear dynamics of a DC battery-charged vibration-to-electricity energy converter. The maximum output power and optimal design under restricted area and voltage were found by resolving the nonlinear equations of movement. To allow the integration with power management circuits, the output voltage is limited to 40 V. Under these conditions, the maximum power was 38.1 μW and 0.87 μW for a device with and without a 4 gr external mass, respectively. The authors concluded that the optimized converters can produce significant power only for a limited range of design and operation parameters. Over certain range of these parameters, the converters could not operate stably.

Paracha et al. (2009) experimentally demonstrated the ability to scavenge the energy of mechanical vibration energy to provide electrical energy to a resistive load by using an electrostatic silicon-based MEMS transducer manufactured in CMOS-compatible technology. Paracha et al. found that the converted power was between 60 μW and 100 μW, for an external vibration of 250 Hz as resonant frequency and amplitude of acceleration of 0.25 g where g is gravitational acceleration 9,81 m/s2. They proposed a novel method for calculating the maximum power that can be produced from a spring-mass system excited with a sinusoidal force, based on the analogy of an electrical impedance network.

Lee et al. (2009) provided a comparison of the capabilities of harvesting energy from three different electrostatic mechanisms and discussed the relationship between the parameters that contribute to maximizing the energy that can be harvested from a micro electro mechanical electrostatic system (MEMS) apparatus. The three mechanisms considered were: the plane-overlap, in plane gap closing and out-of-plane gap closing. Based on the analytical model, the mass of the moving loads and cross-sectional surfaces of the devices active regions were set to

be the same for all devices, while assuming that the electrostatic mechanisms operated in an ideal vacuum environment. Some case studies have shown that an in-plane gap closing structure has the potential to produce a higher amount of energy per unit volume compared to an out-of-plane gap closing mechanism provided that the thickness of the mass of the structure the in plane gap is above the critical value.

Cottone et al. (2013) developed a novel vibration energy harvester design consisting of a double-mass contactless frequency-up converter with buckled clamped-clamped beams aimed at increasing energy harvesting efficiency from low-frequency vibrations. This concept aims at increasing the energy harvesting efficiency for low frequency vibrations. The mechanical to electrical energy conversion was performed through a silicon MEMS micro electrostatic generator based on interdigitated combs. A device prototype was fabricated and experimentally investigated under harmonic frequency sweeping at 0.2 g rms (g = 9.81 m/s2) and band-limited colored noise 0.15 g rms with a pre-charge voltage of 2.5 V. In the buckled-beam bi-stable configuration, the researchers found that the electrostatic generator showed a gain factor of 100 % that mean the harvested power increases of more than 100 times at low frequencies in the interval vibrations between 20 and 50 Hz for the bi-stable mode versus the normal operation mode, despite of the fact that the converter itself was designed to resonate at 162 Hz. Cottone et al. claim that this concept can be applied to different transduction techniques.

Kempitiya et al. (2012) proposed a technique to improve the output power from vibration-based charge-constrained electrostatic ambient energy harvesters. Converting synchronous energy to produce a net energy gain with minimum power dissipation without the need for complex sensing mechanisms is a contribution of the proposed control technique. The energy harvesting

circuit produces a measured power of 1.688 μW for a power investment of 417 nW. The measured power consumption associated with the on-chip controller unit is 24 nW, approximately 1.42 % of the total power harvested. According to Kempitiya et al., this type of micro-watt power generation circuit can be considered for powering communications transceivers and portable electronic devices.

Galayko et al. (2011) investigated the dynamic behaviour of an electrostatic Energy Vibration Harvester (e-HEV) which uses gap-closing capacitive sensors operating in a constant charge mode. The authors studied theoretical insight allowing a quantitative characterization of the highlighted instability phenomena and found that, depending on the amplitude of the external vibrations, three types of pathological behaviour occur at low amplitude, large amplitude and middle amplitude. The study showed that none of this behaviour was similar to that observed for a constant voltage biased capacitive transducer.

Chen et al. (2006) have modelled a new cantilever piezoelectric bimorph transducer converting micro electro-mechanical energy, based on the basic approach. The analysis model showed that the voltage induced by vibration was proportional to the excitation frequency of the device, but inversely proportional to the length of the cantilever beam and the damping factor. Chen et al.'s experimental results indicated that the maximum output voltage differed very slightly from the energy conversion analytical model.

Lu et al. (2011) proposed a new maximum power point (MPP) tracking system to harvest the maximum power from a vibration system. An energy harvesting system based on vibrations and piezoelectric conversion for micro power supply was made and presented. The circuit was fabricated and measurements were carried out to verify the tracking performance and the

feasibility of the proposed platform. The results showed that the power harvesting efficiency of the overall circuit was over 90 %.

Sodano et al. (2004) developed a model of the piezoelectric power harvesting device. The derivation of the model has been provided, allowing it to be applied to a beam with various boundary conditions or layout of piezoelectric patches. The model was verified using experimental results and proved to be accurate independent of the precise frequency of excitation and the load resistance. The measured current generated by the Quick Pack was compared to the predicted current from the model for various frequencies and load resistances. The verification of the model was performed on a structure the contained a complex piezoelectric layout and a non-homogenous material beam, indicating that the model is robust and can be applied to a variety of different mechanical conditions. The damping effects of power harvesting were also shown to be predicted in the model and to follow that of a resistive shunt damping circuit.

Qiu et al. (2009) introduced research activities of vibration control and energy harvesting using piezoelectric materials and a nonlinear approach based on Synchronized Switch Damping (SSD). The SSD technique, also called pulse-switched method, consists in a nonlinear processing of the voltage on a piezoelectric actuator. It is implemented with a simple electronic switch synchronously driven with the structural motion. This switch, which is used to cancel or inverse the voltage on the piezoelectric material, allows to briefly connecting a simple electrical network (short circuit, inductor, voltage sources depending on the SSD version) to the piezoelectric material. Due to this process, a voltage magnification is obtained and a phase shift appears between the strain in piezoelectric patch and the resulting voltage. The force generated by the resulting voltage is always opposite to the velocity of the structure, thus creating net mechanical

energy dissipation. The dissipated energy corresponds to the part of the mechanical energy which is converted into electric energy. Maximizing this energy is equivalent to minimizing the mechanical energy in the structure under given excitation. This process increases the amount of converted electrical energy during a mechanical loading cycle of the piezoelectric material.

Zhou et al. (2012) proposed and investigated a novel piezoelectric energy harvester with a multimode dynamic magnifier capable of significantly increasing the bandwidth and the energy harvested from ambient vibration. The design comprised a multimode intermediate beam with a tip mass, called a dynamic magnifier and an energy harvesting beam with a tip mass. The theoretical analysis is conducted for the coupled beams by considering the interaction of one beam with the other. From the mode shapes of the first six resonant frequencies of the coupled structure drawn from the theoretical and finite element modelling (FEM) analyses, it is shown that the voltage generated by the energy harvesting beam is dramatically magnified in a broad bandwidth and the vibration of the primary beam is mitigated. Zhou et al. experimentally demonstrated that 25.5 times more energy can be harvested in a frequency range of 3 – 300 Hz from the energy harvesting beam by adding a multi-mode dynamic magnifier. The energy harvesting is increased by 100 – 1000 times near these resonances of the harvesting beam.

Patel et al. (2011) proposed a versatile model for optimizing the performance of a rectangular cantilever beam piezoelectric energy harvester used to convert ambient vibrations into electrical energy. The developed model accounts for geometric changes to the natural frequencies, mode shapes, and damping in the structure. This is achieved through the combination of finite element modelling and a distributed parameter electromechanical model, including load resistor and charging capacitor models. The model has the potential for use in investigating the influence of

numerous geometric changes on harvester performance, and incorporates a model for accounting for changes in damping as the geometry changes. The model is used to investigate the effects of substrate and piezoelectric layer length, and piezoelectric layer thickness on the performance of a microscale device. Findings from a parameter study indicate the existence of an optimum sample length due to increased mechanical damping for long beams and improved power output using thicker piezoelectric layers. To achieve unbiased comparisons between different harvester designs, parameter studies are performed by changing multiple parameters simultaneously with the natural frequency held fixed. Performance enhancements were observed using shorter piezoelectric layers as compared to the conventional design, in which the piezoelectric layer and substrate are of equal length.

While the potential of piezoelectric energy harvesting is well established, limitations remain. The most significant challenge is the relatively low power density achievable under typical ambient vibration or stress conditions. This makes piezoelectric harvesters best suited to low-power applications rather than high-energy systems. Additionally, their performance is frequency-dependent, meaning that changes in the vibration spectrum can reduce efficiency. Long-term durability under repeated mechanical loading and environmental exposure is another consideration, as material degradation can reduce performance over time. Addressing these issues often requires careful integration of mechanical, electrical, and material design, as well as consideration of hybrid approaches that combine piezoelectric energy harvesting with other techniques such as electromagnetic or electrostatic conversion. Despite these challenges, research in this field continues to evolve rapidly, driven by the growing need for sustainable, maintenance-free power sources for distributed electronic systems. Advances in materials science, fabrication techniques, and power management electronics are gradually improving the

performance, reliability, and applicability of piezoelectric energy harvesters. These studies demonstrate the importance of both mechanical and electrical optimizations in realizing practical piezoelectric energy harvesting systems. These works, alongside other contributions in the field, form a solid foundation for ongoing innovation and highlight the versatility of piezoelectric generation as a renewable micro-power source for the modern world.

CHAPTER 3

3.1 MATERIALS AND METHODOLOGY

This chapter outlines the methodology and tools employed to model and simulate the piezoelectric footstep energy harvester. The approach focuses on creating a robust simulation environment that allows for quantitative analysis of energy generation under various conditions.

3.1.1 Materials

The simulation of the piezoelectric footstep energy harvester was developed using MATLAB R2024b and its integrated environment, Simulink. These tools were selected for their comprehensive capabilities in mathematical computation, system modeling, and simulation, making them ideal for complex engineering analyses.

3.1.1.1 MATLAB R2024b

MATLAB, which stands for Matrix Laboratory, is a high-level programming language and interactive environment developed by MathWorks for numerical computation, data analysis, and algorithm implementation. Its strength lies in handling matrix-based mathematics, which makes it ideal for tasks like signal processing, data visualization, and writing scripts to automate complex calculations and parameter definition for engineering models. MATLAB R2024b was utilized for:

1. **Parameter Definition:** Defining all essential system parameters, including piezoelectric material properties (permittivity, elasticity), geometric dimensions (crystal thickness, area), electrical characteristics (load/resistance) and simulation-specific variables (number of stacked crystals N).
2. **Data Generation:** Generating realistic footstep force profiles. This involved creating time vectors and corresponding force vectors, simulating discrete footsteps with randomized magnitudes, and generating scaled versions of these profiles to analyze the impact of varying footstep force.
3. **Data Management:** Saving generated force profiles and simulation parameters into `.mat` files, which are directly readable by Simulink.
4. **Post-Processing and Analysis:** Conducting post-simulation analysis of logged data, including calculating total energy harvested and preparing data for plotting.

3.1.1.2 Simulink

Simulink, which runs on MATLAB, is a block diagram environment for multi-domain simulation and Model-Based Design which was used to construct the dynamic system model of the piezoelectric energy harvester. Its graphical interface allows for the intuitive representation of physical systems and their interactions. Key components and functionalities utilized in the model include:

1. **System Modeling:** Building the core model of the piezoelectric energy harvester, which converts mechanical input (footstep force) into electrical output (voltage, power, energy).

2. **Subsystems:** Creating modular subsystems to represent different functional parts of the harvester, such as the mechanical force input, the electromechanical conversion, and the electrical circuit. This promotes a clear, organized model structure.
3. **Signal Generation:** Using "From Workspace" blocks to import the force profile data generated in MATLAB, providing the dynamic mechanical input.
4. **Mathematical Operations:** Employing various blocks for mathematical computations, including multiplication (for parameter scaling and power calculation), division (for stress calculation), and integration (for energy calculation).
5. **Electrical Circuit Simulation:** Modeling essential electrical components such as controlled voltage sources (representing the piezoelectric output), capacitors (modeling internal capacitance), and resistors (representing the load).
6. **Data Visualization:** Utilizing the Scope block for real-time (though often paused for large datasets) visualization of signals during debugging and, more importantly, utilizing Signal Logging for efficient post-simulation data acquisition of time-series outputs like voltage, current, and power.

3.1.2 Methodology

This project employed a Model-Based Design approach using MATLAB and Simulink to quantitatively analyze the performance of a piezoelectric footstep energy harvester. The methodology was structured around three primary comparative studies, each designed to isolate and measure the impact of a single design factor on the system's energy output. A total of 15 distinct simulations were conducted, covering a 5-minute (300-second) period for each scenario.

3.1.2.1 Overall Approach

The core of the methodology was the electromechanical coupling principle, governed by the following equations:

a. Total Voltage (V_{total}): The voltage output from a stack of piezoelectric crystals is a direct function of the applied force (F), area (A), thickness (t) and the material's properties (g33).

$$V_{total} = N \cdot \frac{g33 \cdot t \cdot F}{A} \quad (3.1)$$

b. Instantaneous Power (P): The power generated is a function of the voltage and the load resistance (R_{load}).

$$P = \frac{Vtotal^2}{Rload} \quad (3.2)$$

c. Total Energy (E): The total energy harvested over the simulation period is the time-integral of the instantaneous power.

$$E = \int P dt \quad (3.3)$$

To execute the simulations, a two-part workflow was established: a MATLAB script for parameter definition and data generation, and a Simulink model for system simulation.

3.1.2.2 Data Generation and Parameterization

A custom MATLAB script was developed to create all necessary input data and define the parameters for the simulations. This script served as the central control for the entire project.

a. **Footstep Profiles:** The script generated a base footstep force profile comprising 100 discrete steps over a 300-second period, with a 3-second interval between each step. The peak force of each step was randomized between 400 N and 900 N to simulate the natural variability of human gait. This base profile was then scaled to create four additional profiles, representing 90%, 80%, 70%, and 60% of the original force magnitudes.

b. **Material and Geometric Parameters:** The script defined all material-specific constants, such as g33 for the five selected materials, as well as the fixed geometric parameters of the crystals (thickness, radius) and the standard load resistance. This approach allowed for quick and reproducible changes between simulation runs.

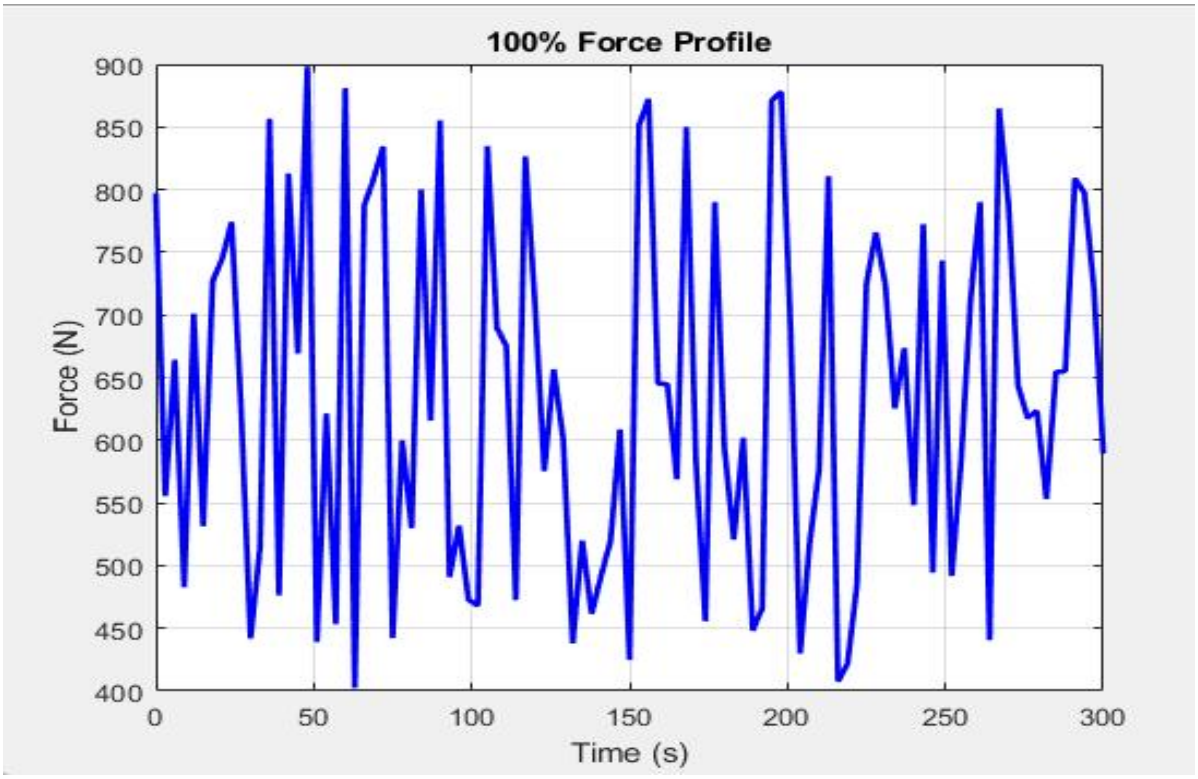

Figure 3.1: Generated force profile.

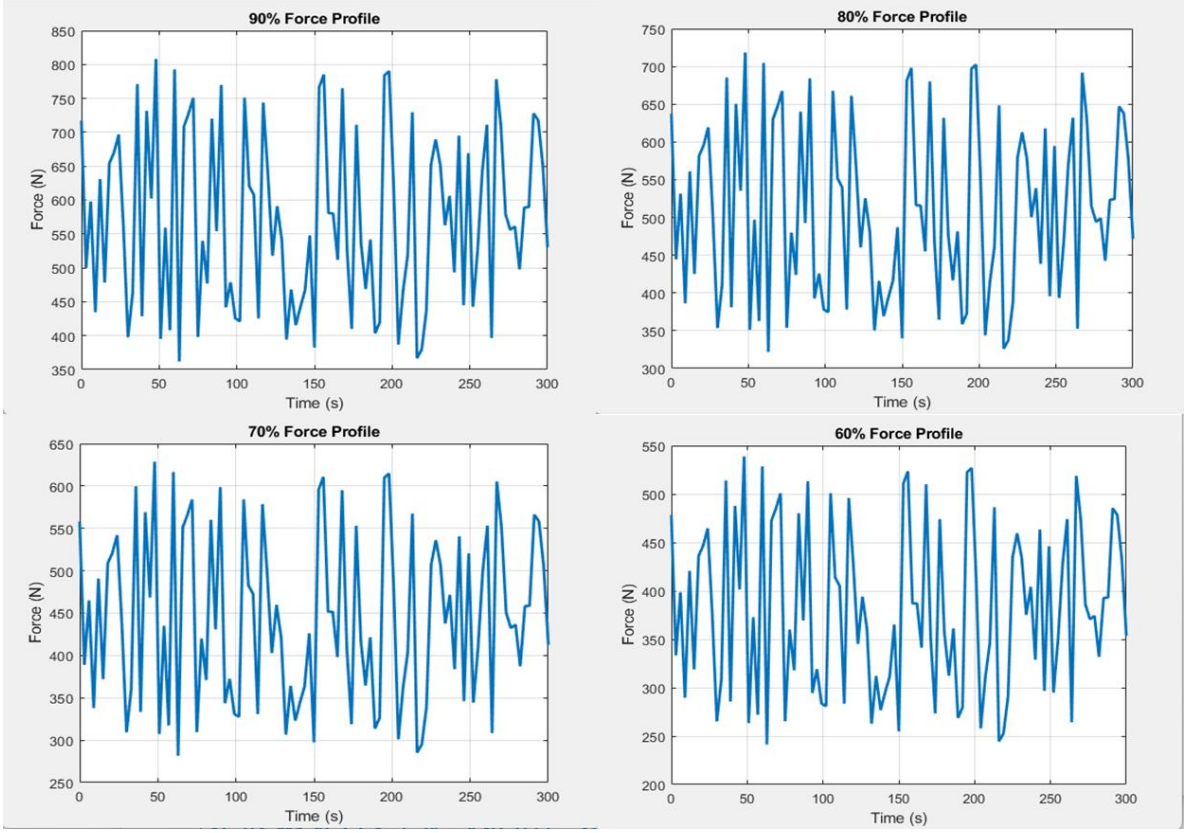

Figure.3.2: Scaled force profiles

3.1.2.3 Simulink Model Breakdown

The Simulink model was designed as a block diagram that directly represents the governing equations of the harvester

1. **Force Input:** A 'From' Workspace block was used to import the `time` and `force` vectors generated by the MATLAB script. This block acts as the dynamic input to the system, providing the time-series force data.
2. **Voltage Calculation Subsystem:** This subsystem directly implemented the voltage equation.

a. **Constant Blocks:** Separate Constant blocks were used to represent the material properties (g_{33}), crystal dimensions (t_{cry} and A_{cry}), and the number of crystals in the stack (N). This setup facilitated easy modification of parameters for each comparative study.

b. **Product and Divide Blocks:** A Divide block calculated the stress ($\sigma = F/A$), while Product blocks multiplied the stress by the constants (g_{33} and t) to determine the open-circuit voltage (VOC). The total voltage (V_{total}) was then calculated by a Gain block representing the number of stacked crystals (N).

3. **Power and Energy Calculation:**

a. **Function Block:** The total voltage signal was fed into a Function block that squared the value (u^2) to calculate power.

b. **Divide Block:** The squared voltage was divided by a Constant block representing the load resistance (R_{load}) to calculate instantaneous power (P).

c. **Integrator Block:** The instantaneous power signal was connected to an Integrator block to compute the total energy harvested (E) over the entire simulation period.

4. **Data Visualization and Logging:**

a. **Scopes:** Scope blocks were connected to key signals (voltage, power) to visually inspect the waveforms. For long simulations, the scope was used for debugging, while Signal Logging was enabled to save all data to the MATLAB workspace for more comprehensive analysis.

b. **Display Block:** A Display block was used to show the final numerical value of the total energy harvested at the end of each simulation run.

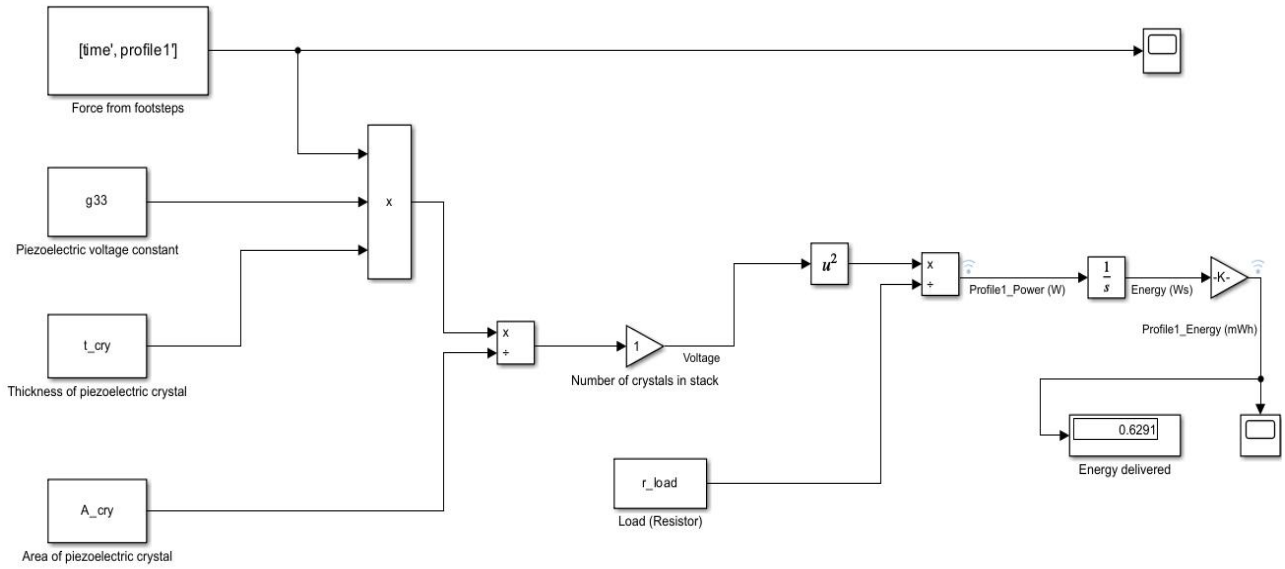

Figure 3.3: Simulink setup of the piezoelectric governing equation

3.1.2.4 Comparative Simulations

The three comparative studies were conducted by systematically altering the parameters in the MATLAB script before each of the 15 simulation runs.

1. **Footstep Magnitude Comparison (5 simulations):** The force vector was changed for each simulation to use one of the five scaled profiles (100%, 90%, 80%, 70%, 60%). All other parameters (stacking, material) were kept constant to isolate the effect of force.
2. **Crystal Stacking Comparison (5 simulations):** The N parameter was varied from 1 to 5, and the base 100% force profile was used for each simulation. This demonstrated the direct impact of stacking on energy output.

3. **Piezoelectric Material Comparison (5 simulations):** The g33 parameter was systematically changed to the value corresponding to each of five selected piezoelectric materials;

    a. Lead Zirconate Titanate (PZT-5A) (g33 = 24.8e-3)
    b. Lead Zirconate Titanate (PZT-5H) (g33 = 26.5e-3)
    c. Barium Titanate (BT) (g33 = 12.5e-3)
    d. Polyvinylidene Fluoride (PVDF) (g33 = 25e-3)
    e. Lead Magnesium Niobate-Lead Titanate (PMN-PT) (g33 = 45e-3)

The base force profile and a fixed number of crystals were used to provide isolate the effect of the different piezoelectric materials hence providing a fair comparison.

CHAPTER 4

RESULTS AND DISCUSSIONS

The results of the simulation were analyzed by focusing on two primary performance metrics: instantaneous power and total harvested energy. These outputs were visualized to provide a clear comparison across all scenarios. For each of the three comparative studies, the results were plotted on single graphs to aid in a comprehensive understanding of the performance differences.

4.1 Data Visualization

All simulation results were analyzed over the 5-minute (300-second) duration. The two main outputs were:

1. **Instantaneous Power (in Watts):** This metric represents the power generated by the harvester at any given moment. It was obtained by calculating the voltage squared divided by the load resistance ($P=V^2/R_{load}$). The power waveforms for each comparison were plotted on a single graph of Power (W) versus Time **(s)** to show the dynamic performance.
2. **Total Energy (in milliwatt-hours):** This is the cumulative energy harvested over the entire 5-minute period. It was calculated by integrating the instantaneous power signal over time. The results for each comparison were plotted on a single graph of Energy (mWh) versus Time (s) to clearly demonstrate the total energy yield. The final value at the end of the simulation was also recorded for a direct numerical comparison.

This dual-visualization approach provided both a dynamic view of the harvester's performance and a final, quantifiable metric for judging its overall effectiveness under different conditions.

4.2 Analysis of Results

4.2.1 Footstep (Force) Magnitude

The analysis of the footstep profile comparison provides a clear and quantitative understanding of the relationship between the magnitude of the applied mechanical force and the harvester's electrical energy output. The results, as summarized in Table 4.1, demonstrate that a decrease in footstep force leads to a corresponding decrease in total harvested energy, with this reduction becoming progressively more significant with each incremental decrease in force.

Table 4.1:

Footstep (Force) Profiles	Total Energy Delivered (mWh)	Percentage Change
100% Force	0.6628	-
90% Force	0.5369	19% Decrease
80% Force	0.4242	21% Decrease
70% Force	0.3248	23.4% Decrease
60% Force	0.2386	26.54% Decrease

Footstep profile comparison

As illustrated in the table, a 10% reduction in the footstep force profile from 100% to 90% resulted in a 19% decrease in total energy output. A subsequent 10% reduction (from 90% to 80%) caused an even larger percentage drop of 21%. This pattern continued with each profile,

culminating in a 26.54% decrease in energy when the force was reduced from 70% to 60%. This numerical trend directly confirms the non-linear, quadratic relationship inherent in piezoelectric energy harvesting, where power is proportional to the square of the applied force ($P \propto F^2$). A small decrease in force leads to a disproportionately larger decrease in the resulting energy.

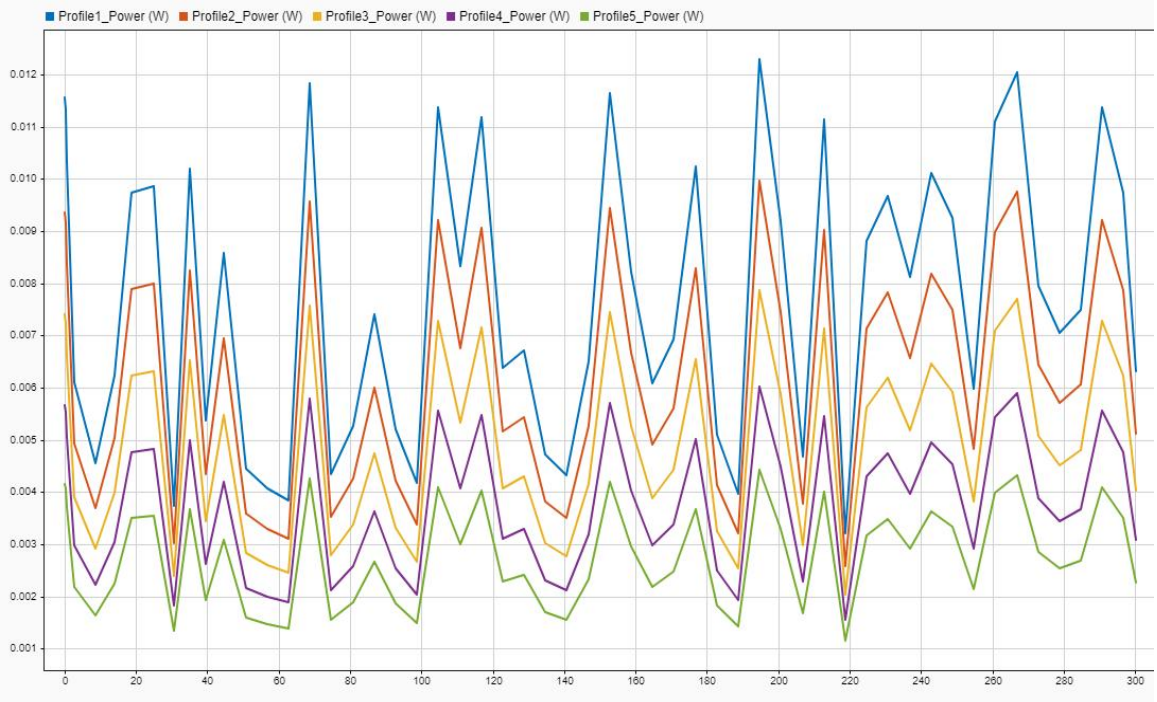

Figure.4.1: Power vs time graph of compared footstep profiles

The power-versus-time graph, depicted in figure 4.1 above, provides a detailed visual representation of this relationship. The graph shows five distinct power profiles, each corresponding to a different scaled footstep input. The peaks of each profile are consistently separated, with the blue line (100% force) showing the highest peak power outputs, followed sequentially by the orange (90%), yellow (80%), purple (70%), and green (60%) lines. This visualization clearly demonstrates that a reduction in force significantly lowers the instantaneous power output, as dictated by the squared relationship.

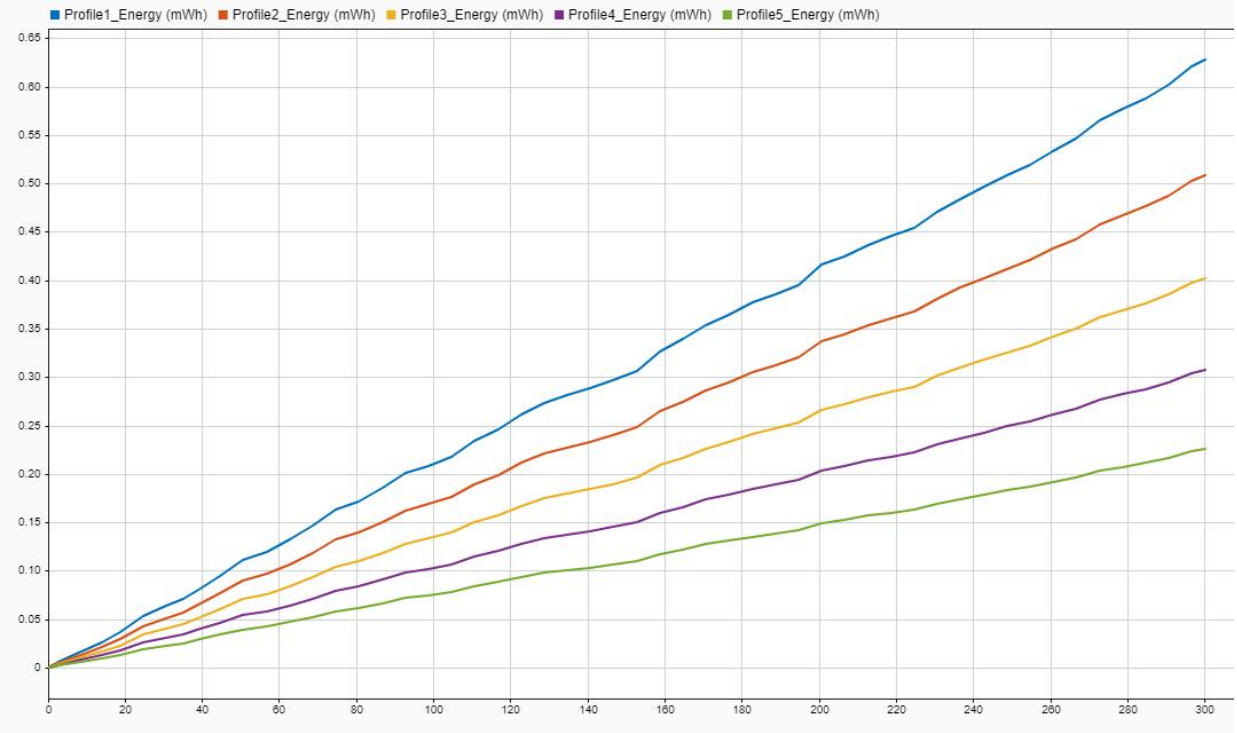

Figure 4.2: Energy vs time graph of compared footstep profiles

Similarly, the energy-versus-time graph, shown in Figure 4.2, further illustrates this behavior in a cumulative manner. While all profiles show a positive, increasing energy trend over the 300-second period, the slope of each line directly corresponds to the average power of the footstep profile. The blue line (100% force) exhibits the steepest slope, indicating the highest rate of energy harvesting. Conversely, the green line (60% force) has the shallowest slope, representing the lowest rate. The final energy values at the 300-second mark on the graph align with the numerical results from the table, confirming the total energy harvested for the 60% force profile is a fraction of the energy harvested by the 100% force profile. These graphs, read in conjunction with the numerical data, provide a comprehensive view of the performance impact of varying footstep magnitudes.

4.2.2 Number of Stacked Crystals

The analysis of the number of stacked crystals provides important insights into the design trade-offs for a piezoelectric energy harvester. The simulation results, as summarized in Table 4.2, confirm that increasing the number of crystals in a series stack leads to a substantial increase in total energy delivered. However, it also reveals a key non-linear behavior: while energy increases with each added crystal, the percentage increase in energy delivered diminishes as more crystals are added.

Table 4.2:

Number of Stacked Crystals	**Total Energy Delivered (mWh)**	**Percentage Change**
1	0.6628	-
2	2.651	75% Increase
3	5.965	55.55% Increase
4	10.6	43.73% Increase
5	16.57	36% Increase

Number of crystals - comparison

As shown in Table 4.2, doubling the number of crystals from one to two resulted in a dramatic 75% increase in total energy. However, the subsequent addition of a third crystal yielded a smaller percentage increase of 55.55%, and by the time the stack reached five crystals, the

percentage increase had dropped to 36%. This trend suggests that while the total energy continues to climb, the efficiency gains per added crystal begin to decrease. This could indicate a practical limit to stacking, where the added complexity, cost, and physical size of including more crystals may not be justified by the diminishing returns in performance.

The power-versus-time graph, shown in Figure 4.3 below, provides a visual explanation for this trend. The graph displays a clear pattern where each successive line represents a higher power output, directly correlating with an increasing number of crystals. The height of the power peaks increases dramatically as the number of crystals grows, confirming the expected quadratic relationship between the number of crystals and power output ($P \propto N^2$). The separation between the power peaks for N=1 and N=2 is much smaller than the separation between N=4 and N=5, visually representing the diminishing gains in energy output with each added crystal.

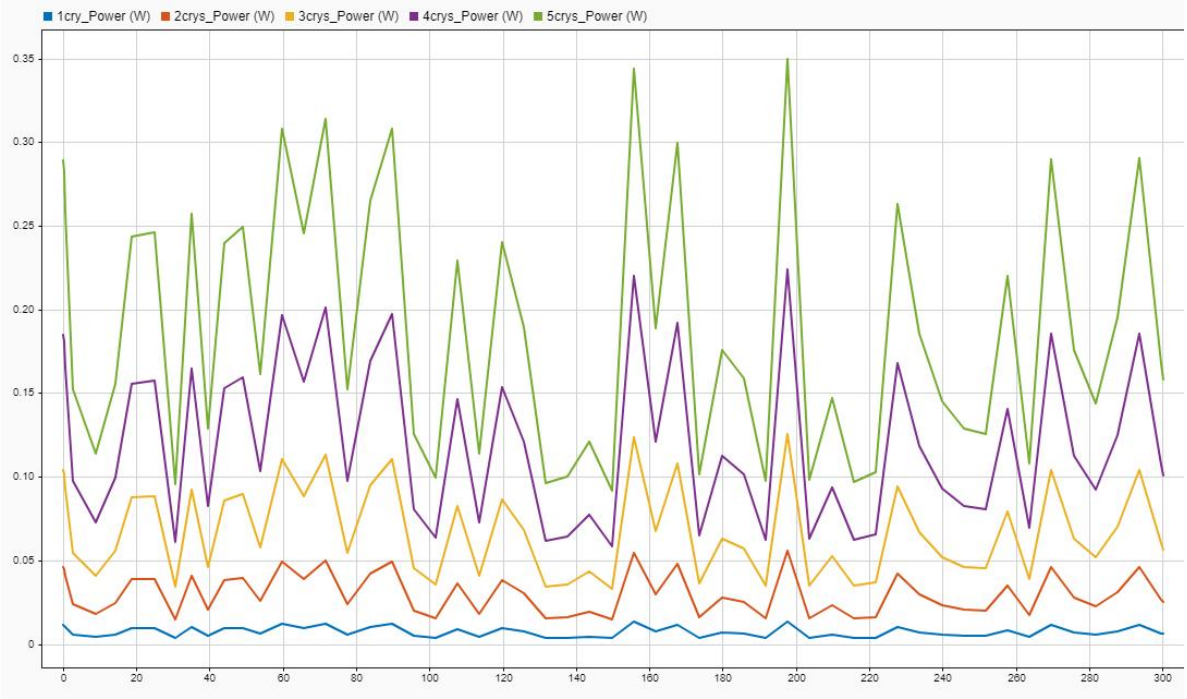

Figure 4.3: Power vs time graph of compared number of stacked crystals

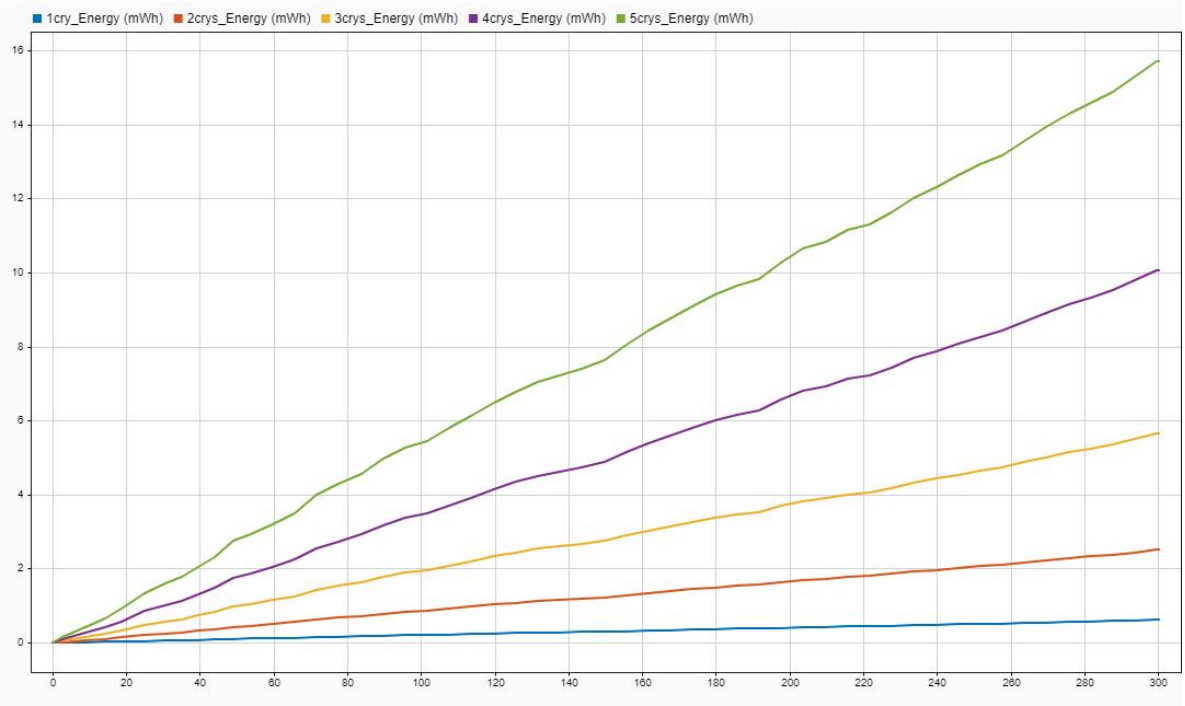

Figure 4.4: Energy vs time graph of compared number of crystals

The energy-versus-time graph, shown in Figure 4.4 above, further highlights this phenomenon in a cumulative manner. The slope of each line represents the rate of energy harvesting. While all lines show a positive trend, the slope for the N=5 line is much steeper than for the N=1 line, confirming its superior performance. However, upon closer inspection, the increase in slope from N=1 to N=2 is visually greater than the increase in slope from N=4 to N=5. This graphical representation reinforces the numerical data, demonstrating that the energy gains diminish with each additional crystal, a crucial consideration for optimizing the design of a real-world energy harvester.

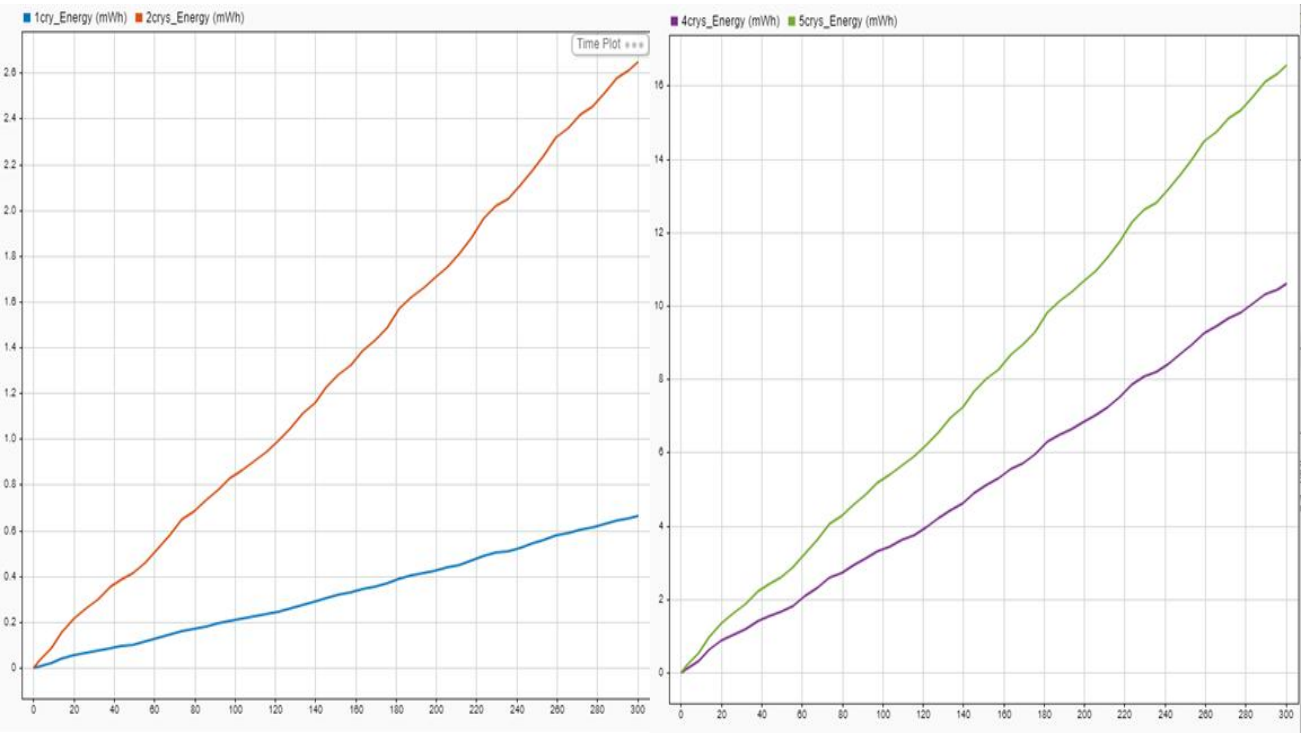

Figure 4.5: Energy gains from N=1 to N=2 compared with energy gains from N=4 to N=5

4.2.3 Piezoelectric Material Comparisons

The selection of the piezoelectric material is an essential design factor that has a significant impact on the harvester's performance. The simulations conducted for this analysis provide a direct, quantitative comparison of five common materials under identical conditions (same footstep profile, stack size, and load). The results, summarized in Table 4.2.3, clearly establish a performance hierarchy based on the material's piezoelectric voltage constant (g_{33}).

Table 4.2:

Piezoelectric Materials	Total Energy Delivered (mWh)	Ranking
Lead Zirconate Titanate (PZT-5A)	0.5805	4th
Lead Zirconate Titanate (PZT-5H)	0.6628	2nd
Barium Titanate (BT)	0.1475	5th
Polyvinylidene Fluoride (PVDF)	0.5899	3rd
Lead Magnesium Niobate-Lead Titanate (PMN-PT)	1.911	1st

Piezoelectric materials comparison

As shown in Table 4.2.3, Lead Magnesium Niobate-Lead Titanate (PMN-PT) emerged as the top-performing material, delivering a total of 1.911 mWh, which is significantly higher than all other materials tested. This performance is directly attributable to its exceptionally high g33 value, a measure of its ability to convert mechanical stress into voltage. PZT-5H, with its high g33 value, ranked second, while PVDF and PZT-5A, with similar g33 values, delivered comparable energy outputs, ranking third and fourth, respectively. Barium Titanate (BT) demonstrated the lowest energy output, a result consistent with its significantly lower g33 value.

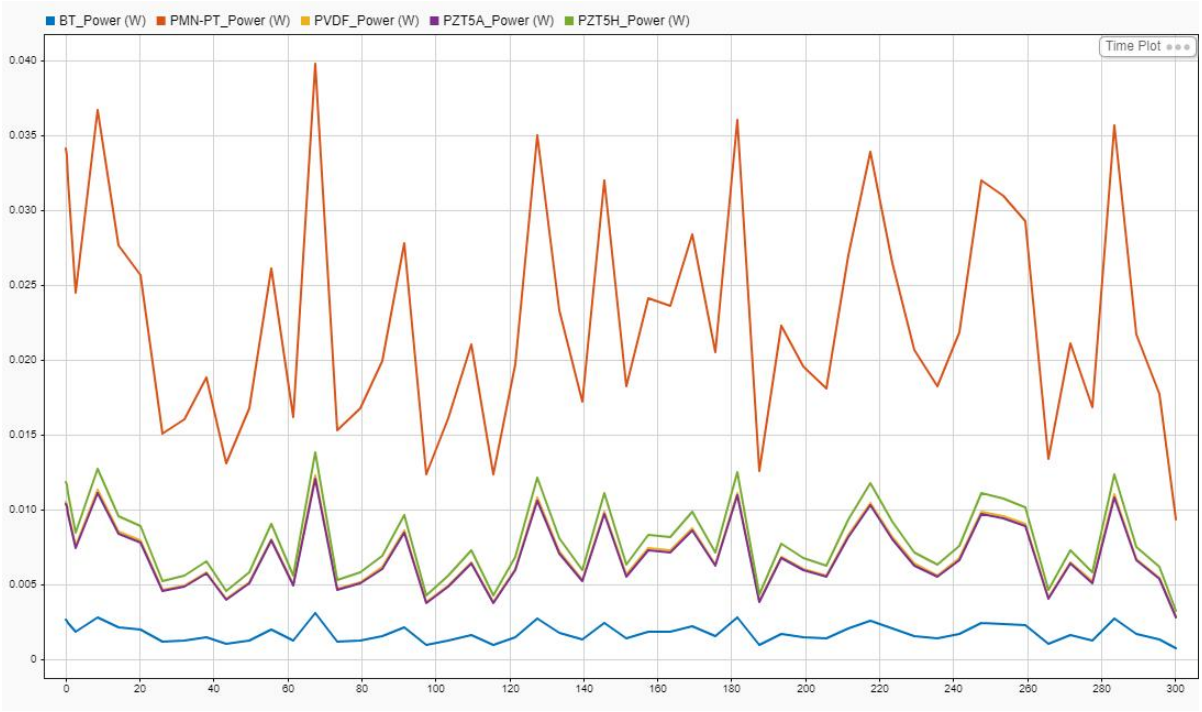

Figure 4.6: Power vs time graph comparing various piezoelectric materials

The power-versus-time graph, depicted above, visually confirms these findings. The graph shows a distinct separation of power profiles, with the PMN-PT (orange line) consistently achieving the highest instantaneous power peaks throughout the simulation. The PZT-5H (green line) maintains the second-highest power output, followed by PVDF (yellow) and PZT-5A (purple), which track closely together. The Barium Titanate (blue line) consistently shows the lowest power output, with its peaks barely registering compared to the other materials.

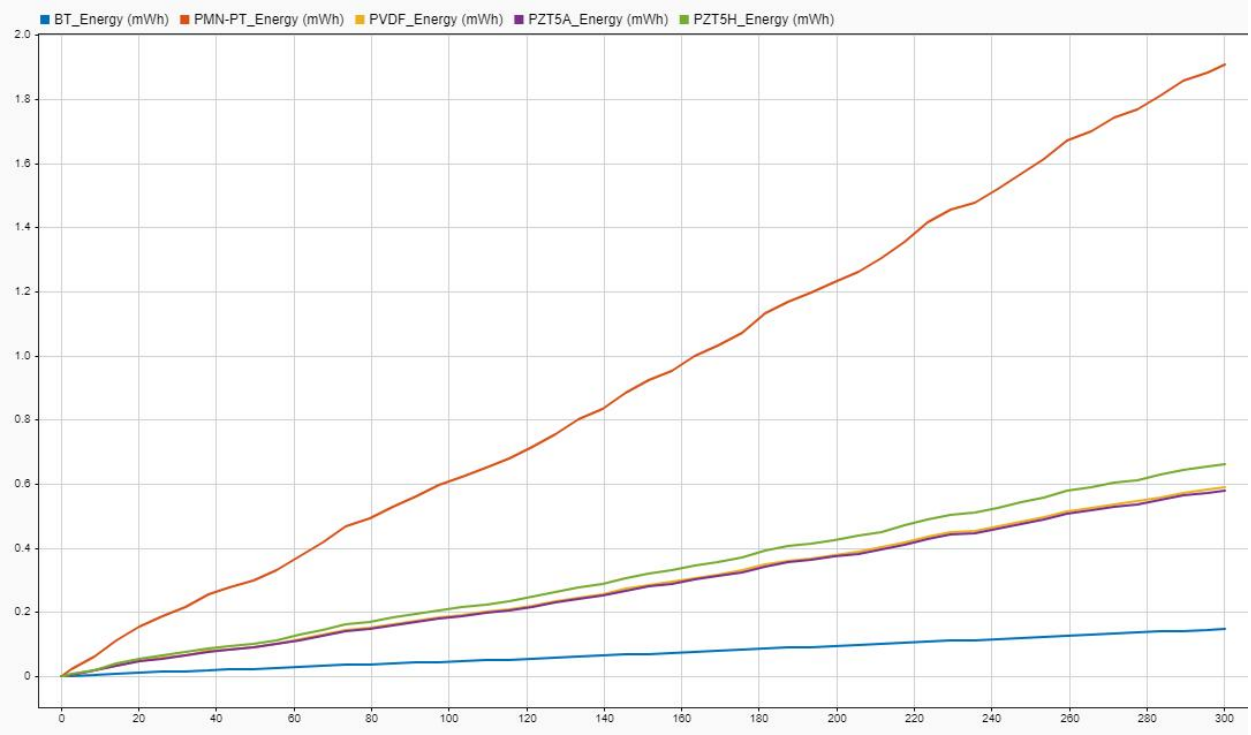

Figure 4.7: Energy vs time graph comparing different piezoelectric materials

The cumulative energy-versus-time graph, shown above, reinforces the hierarchy of material performance. The slope of each line represents the rate of energy harvesting, with the PMN-PT line (orange) having the steepest slope, indicating the fastest energy accumulation. The other materials follow in descending order of slope, matching their respective rankings from the table. The significant gap between the PMN-PT line and the other materials highlights its superior performance for this application. This analysis concludes that material selection is a primary and critical factor in the design of a piezoelectric energy harvester and can lead to a substantial improvement in overall energy output.

CHAPTER 5

CONCLUSION AND RECOMMENDATIONS

This project successfully modeled and simulated a piezoelectric footstep energy harvester, providing a quantitative framework for understanding the system's performance under varying design conditions. The results from the three comparative studies validate key theoretical principles and offer significant insights into the practical design and optimization of such devices.

The analysis of footstep magnitude confirmed the quadratic relationship between force and power ($P \propto F^2$). The simulations demonstrated that a small increase in force leads to a disproportionately larger increase in harvested energy. This finding is crucial for real-world applications, as it suggests that devices placed in high-traffic areas or locations with high-impact footfalls (e.g., stairs, turnstiles, dance floors) would yield significantly more power than those in low-traffic areas.

The study on crystal stacking revealed a powerful method for increasing energy output. The simulations confirmed that while voltage increases linearly with the number of stacked crystals, the total harvested energy increases with the square of the number of crystals ($E \propto N^2$). This implies that stacking is an extremely effective strategy for boosting performance. However, the analysis also showed that the percentage gain in energy diminishes with each added crystal, indicating a point of diminishing returns. This is a vital consideration for design, as it helps determine the optimal balance between performance, cost, and physical size.

Finally, the material comparison highlighted the critical role of material selection. The simulation results established a clear performance hierarchy directly tied to the materials' piezoelectric voltage constants (g33). Materials with higher g33 values, such as PMN-PT, consistently outperformed others, delivering substantially more energy under identical conditions. This demonstrates that investing in higher-performance materials is a primary pathway to maximizing energy output, even at a potentially higher cost.

5.1 Observations

Based on the simulation results, the most effective methods for maximizing the performance of a piezoelectric footstep energy harvester can be ranked by their impact on energy output.

1. **Material Selection:** This is the most critical factor. The analysis demonstrated that a superior material like PMN-PT can yield significantly more energy than other options, even with identical force and stacking conditions. Selecting a material with a high piezoelectric voltage constant (g33) provides the largest performance gain.
2. **Crystal Stacking:** Stacking is a highly effective method for increasing energy output, as the harvested energy scales with the square of the number of crystals ($E \propto N^2$). However, this method has a point of diminishing returns, and its implementation must balance performance gains against increased cost, complexity, and physical size.
3. **Footstep Magnitude:** While a critical factor, footstep force is often an uncontrollable variable. The quadratic relationship ($P \propto F^2$) means that deploying the harvester in high-traffic, high-impact areas (e.g., stairs, entryways) is essential for maximizing yield.

5.2 Improving Harvester Performance

To further improve the performance of a piezoelectric energy harvester, focus should be on enhancing the key parameters identified in this study:

1. **Increasing Force:** One of the main limitations is the variability and magnitude of human footsteps. To address this, mechanical amplification mechanisms can be integrated into the harvester's design. This could involve a lever system or a spring-loaded mechanism that concentrates the force from a wide, distributed footfall onto a smaller area of the piezoelectric crystal. Such a system could enable a light footstep to transmit a much greater, more focused force to the crystal, thereby significantly increasing voltage and power output.
2. **Optimizing Material Use:** While PMN-PT offers superior performance, it is often a single-crystal, high-cost material. A viable alternative could be to use PZT ceramics (e.g., PZT-5H), which offer a good balance of high performance, lower cost, and easier manufacturing. Further research could explore lead-free alternatives to address environmental concerns associated with PZT.

5.3 General Recommendations

Based on the comprehensive analysis of the simulation results, several key recommendations can be made to optimize the design and deployment of a piezoelectric footstep energy harvester.

1. **Prioritize Material Selection**: The most significant performance gains were achieved by using a material with a high piezoelectric voltage constant, g_{33} . While PMN-PT offered the highest energy yield in the simulations, its high cost and brittle nature may be

prohibitive for large-scale applications. A practical recommendation is to use PZT-5H, which provides an excellent balance of high performance and greater durability and is a well-established ceramic.

2. **Optimize Crystal Stacking**: Stacking is a highly effective method for boosting voltage and power output, as energy scales with the square of the number of crystals. However, the analysis showed a point of diminishing returns in percentage gain for each added crystal. Therefore, the optimal design should carefully balance the number of crystals to achieve sufficient energy output without excessive cost or bulk.
3. **Enhance Mechanical Amplification**: To overcome the limitation of variable footstep force, consider integrating a mechanical amplification mechanism into the harvester. A lever or spring-loaded system can concentrate the force from a larger area of a footfall onto the smaller surface area of the crystal, significantly boosting the transmitted stress and thus, the voltage and power output. This would make the harvester more effective even with lighter footsteps or in low-traffic areas.
4. **Target Strategic Deployment Locations**: Since harvested power is proportional to the square of the applied force, the harvester's location is critical. The device should be deployed in high-traffic, high-impact areas such as stairs, entryways, or turnstiles to maximize its energy yield.

5.4 Project Limitations and Considerations

Despite the detailed analysis, the simulated model has certain limitations that should be addressed in future work. The model assumes ideal conditions, such as:

1. **Ideal Electrical Load:** A fixed resistive load was used, while real-world applications would require a more complex power management circuit (e.g., rectifiers and storage capacitors) to capture and store energy.
2. **Constant Force Application:** The discrete model of force, while effective, does not capture the full, continuous force profile of a real footstep, which could include vibration and dynamic stress.
3. **Material Limitations:** The model did not account for material fatigue, hysteresis, or temperature effects, which can degrade performance over time. Certain materials, like PMN-PT, are highly effective but may be too brittle or expensive for large-scale production and installation.

5.5 Areas for Future Research

The current model provides a strong foundation but has limitations that can be addressed in future work. A more advanced model could incorporate a dedicated power management circuit, including a rectifier and a storage capacitor, to better simulate a real-world system. Additionally, future studies should consider material degradation over time, fatigue, and environmental factors such as temperature, which could affect performance. Investigating lead-free piezoelectric materials could also provide a more environmentally friendly solution for widespread use

In conclusion, the findings from this study provide a robust, data-driven foundation for the design of an efficient piezoelectric footstep energy harvester. The results collectively indicate that a high-yield device should:

1. Be deployed in environments with high footfall forces.
2. Utilize a carefully selected number of stacked crystals to balance performance with cost.
3. Be constructed with a high-performance piezoelectric material like PMN-PT to maximize energy conversion efficiency.

These insights move the concept of a piezoelectric harvester from a theoretical possibility to a well-understood and optimizable engineering solution.

REFERENCES

1. AboutPavegen. (n.d.). *How it all started*. Consultato 5 Settembre 2021. Retrieved March 25, 2025, from https://pavegen.com/ar/about/

2. Ahmad, A. F., Razali, A. R., Romlay, F. R. M., & Razelan, I. S. M. (2021). Energy harvesting on pavement: A review. *International Journal of Renewable Energy Research (IJRER)*, 11, 1250–1266.

3. Ahmad, S., Abdul Mujeebu, M., & Farooqi, M. A. (2019). Energy harvesting from pavements and roadways: A comprehensive review of technologies, materials, and challenges. *International Journal of Energy Research*, 43, 1974–2015.

4. Asef Ishraq Sadaf, Riaz Ahmed* and Hossain Ahmed. (2024) *Cantilever configurations in vibration-based piezoelectric energy harvesting: a comprehensive review on beam shapes and multi-beam formations*

5. Beeby, S. P., Torah, R. N., Tudor, M. J., Jones, P. G., O'Donnell, T., & Saha, C. R. (2007). A micro electromagnetic generator for vibration energy harvesting. *Journal of Micromechanics and Microengineering*, 17, 1257–1265.

6. Chen, S. N., Wang, G. J., & Chien, M. C. (2006). Analytical modelling of piezoelectric vibration-induced micro power generator. *Mechatronics*, 16, 379–387.

7. Chiu, Y., & Chang, C. F. (2010). Modelling and analysis of a DC electrostatic vibration-to-electricity micro power generator. *PowerMEMS*, 1–4.

8. Cottone, F., Basset, P., Guillemet, R., Galayko, D., Marty, F., & Bourouina, T. (2013). Bistable multiple-mass electrostatic generator for low-frequency vibration energy harvesting. *IEEE MEMS*, 861–864.

9. Damjanovic, D. (2025). *Encyclopedia of condensed matter physics*. Retrieved August 3, 2025, from https://www.sciencedirect.com/referencework/9780123694010/encyclopedia-of-condensed-matter-physics

10. Elhalwagy, A. M., Ghoneem, M. Y. M., & Elhadidi, M. (2017). Feasibility study for using piezoelectric energy harvesting floor in buildings' interior spaces. *Energy Procedia*, 115, 114–126.

11. Galayko, D., Guillemet, R., Dudka, A., & Basset, P. (2011). Comprehensive dynamic and stability analysis of electrostatic vibration energy harvester (E-VEH). *IEEE Transducers*, 11, 2382–2385.

12. Kempitiya, A., Borca-Tasciuc, D. A., & Hella, M. M. (2012). Low power ASIC for microwatt electrostatic energy harvesters. *IEEE Transactions on Very Large Scale Integration (VLSI) Systems*, 12, 5639–5647.

13. Lee, C., Lim, Y. M., Yang, B., Kotlanka, R. K., Heng, C. H., & He, J. H. (2009). Theoretical comparison of the energy harvesting capability among various electrostatic mechanisms from structure aspect. *Sensors and Actuators A: Physical*, 156, 208–216.

14. Li, W. J., Ho, T. C. H., Chan, G. M. H., Leong, P. H. W., & Wong, H. Y. (2000). Infrared signal transmission by a laser-micromachined, vibration-induced power generator. *Proceedings of the IEEE Midwest Circuits and Systems Conference*, 1, 236–239.

15. Lu, C., Tsui, C. Y., & Ki, W. H. (2011). Vibration energy scavenging system with maximum power tracking for micro power applications. *IEEE Transactions on Very Large Scale Integration (VLSI) Systems*, 19, 2109–2119.

16. Maung, P. P. (2022). *Design and construction of piezoelectric power generation system* (Bachelor's thesis). Yangon Technological University.

17. Paracha, A. M., Basset, P., Galayko, D., Dudka, A., Marty, F., & Bourouina, T. (2009). MEMS DC/DC converter for 1D and 2D vibration-to-electricity power conversion. *IEEE Transducers*, 2098–2101.

18. Patel, R., McWilliam, S., & Popov, A. A. (2011). A geometric parameter study of piezoelectric coverage on a rectangular cantilever energy harvester. *Smart Materials and Structures*, 20.

19. Qiu, J. H., Ji, H. L., & Shen, H. (2009). Energy harvesting and vibration control using piezoelectric elements and a nonlinear approach. *IEEE International Symposium on the Application of Ferroelectrics*, 18, 1–8.

20. Sadaf, A. I., Ahmed, R., & Ahmed, H. (2024). Cantilever configurations in vibration-based piezoelectric energy harvesting: A comprehensive review on beam shapes and multi-beam formations.

21. Sodano, H. A., Park, G., & Inman, D. J. (2004). Estimation of electric charge output for piezoelectric energy harvesting. *Journal of Strain Analysis*, 40, 49–58.

22. Wang, P., Liu, H., Dai, X., Yang, Z., Wang, Z., & Zhao, X. (2012). Design, simulation, fabrication and characterization of a micro electromagnetic vibration energy harvester with sandwiched structure and air channel. *Microelectronics Journal*, 43, 154–159.

23. Williams, C. B., Shearwood, C., Harradine, M. A., Mellor, P. H., Birch, T. S., & Yates, R. B. (2001). Development of an electromagnetic micro-generator. *IEE Proceedings - Circuits, Devices and Systems*, 148, 337–342.

24. Zhou, W. L., Penamalli, G. R., & Zuo, L. (2012). An efficient vibration energy harvester with a multi-mode dynamic magnifier. *Smart Materials and Structures*, 21.

APPENDIX:

Matlab Code:

```
% MATLAB script for piezoelectric system

% --- Parameters ---
total_time = 300;         % Total duration in seconds
step_interval = 3;        % Time between steps (seconds)
num_steps = total_time / step_interval; % Number of steps

% --- Create the Time Vector and Base Force Profile ---
% The time vector will have a point for each step
time = 0:step_interval:total_time;

% Initialize an empty force vector
base_force = zeros(size(time));
min_force = 400;          % Minimum force (Newtons)
max_force = 900;          % Maximum force (Newtons)

for i = 1:length(time)
    % Generate a random force for each step
    base_force(i) = min_force + (max_force - min_force) * rand();
end


% --- Scale the Base Profile to Create Four More Profiles ---
profile1 = base_force;              % 100% of base force
```

```
profile2 = base_force * 0.90;       % 90% of base force
profile3 = base_force * 0.80;       % 80% of base force
profile4 = base_force * 0.70;       % 70% of base force
profile5 = base_force * 0.60;       % 60% of base force


% Plot 100% Force Profile
figure;
plot(time, profile1, 'b', 'LineWidth', 2);
title('100% Force Profile');
xlabel('Time (s)');
ylabel('Force (N)');
grid on;

% Plot 90% Force Profile
figure;
plot(time, profile2, 'LineWidth', 2);
title('90% Force Profile');
xlabel('Time (s)');
ylabel('Force (N)');
grid on;

% Plot 80% Force Profile
figure;
plot(time, profile3, 'LineWidth', 2);
title('80% Force Profile');
xlabel('Time (s)');
ylabel('Force (N)');
```

```
grid on;

% Plot 70% Force Profile
figure;
plot(time, profile4, 'LineWidth', 2);
title('70% Force Profile');
xlabel('Time (s)');
ylabel('Force (N)');
grid on;

% Plot 60% Force Profile
figure;
plot(time, profile5, 'LineWidth', 2);
title('60% Force Profile');
xlabel('Time (s)');
ylabel('Force (N)');
grid on;



%Assign values to parameters

N = 1;                          %Number of crystals in stack
r_cry = 0.025;                  %Radius of a single crystal(m)
A_cry = pi*(r_cry^2);           %Area of a single crystal(m)
t_cry = 0.01;                   %Thickness of a single crystal(m)
g33 = 26.5*(10^-3);             %Piezoelectric voltage constant of the material
r_load = 1*10^6;                %Resistance load (ohms)
```

```
g33_p5a = 24.8*(10^-3);          %Lead Zirconate Titanate (PZT-5A)

g33_p5h = 26.5*(10^-3);          %Lead Zirconate Titanate (PZT-5H)

g33_bt = 12.5*(10^-3);           %Barium Titanate (BT)

g33_pvdf = 25*(10^-3);           %Polyvinylidene Fluoride (PVDF)

g33_pmn = 45*(10^-3);            %Lead Magnesium Niobate-Lead Titanate (PMN-PT)
```